MOSS, S. C. & CLAPP, P. C. (1968). *Phys. Rev.* **171**, 764–777.
MOZER, B., KEATING, D. T. & MOSS, S. C. (1968). *Phys. Rev.* **175**, 868–876.
OHSHIMA, K., WATANABE, D. & HARADA, J. (1976). *Acta Cryst.* A**32**, 883–892.
ROTH, L. M., ZEIGER, H. J. & KAPLAN, T. A. (1966). *Phys. Rev.* **149**, 519–525.
SCHOLZ, G. A. & FRINDT, R. F. (1980). *Mater. Res. Bull.* **15**, 1703–1716.
SUTER, R. M., SHAFER, M. W., HORN, P. M. & DIMON, P. (1982). *Phys. Rev. B*, **26**, 1495–1498.
THOMPSON, A. H. (1978). *Phys. Rev. Lett.* **40**, 1511–1514.
TIBBALS, J. E. (1975). *J. Appl. Cryst.* **8**, 111–114.
UNGER, W. K., REYES, J. M., SINGH, O., CURZON, A. E., IRWIN, J. C. & FRINDT, R. F. (1978). *Solid State Commun.* **28**, 109–112.
WALKER, C. B. & KEATING, D. T. (1961). *Acta Cryst.* **14**, 1170–1176.

Acta Cryst. (1983). A**39**, 305–310

Secondary Extinction Factor for Spherical Crystals

BY T. KAWAMURA AND N. KATO

Department of Crystalline Materials Science, Faculty of Engineering, Nagoya University, Chikusa-ku, Nagoya, Japan

(*Received* 10 *September* 1982; *accepted* 22 *November* 1982)

Abstract

The extinction factor η was numerically calculated for spherical crystals based on the new statistical dynamical theory [Kato (1976). *Acta Cryst.* A**32**, 458–466]. The optical paths in the Bragg case and other geometrical cases such as the Laue–Bragg–Laue are properly treated, so that the accuracy is estimated to be 0·1% for $\mu_0 R \leq 3{\cdot}0$, $\sigma R \leq 2{\cdot}0$ and $\theta_B \leq 30°$ (μ_0 absorption coefficient, σ the coupling constant of the energy transfer equations, θ_B the Bragg angle). Based on these calculations a universal fitting function $\eta(\mu_0 R, \sigma R, \theta_B)$ is proposed in the above-mentioned domains. The accuracy is better than 0·4% if η is larger than 10%. The difference between the present and the conventional theories is significant if the extinction exceeds 20%.

1. Introduction

One of the authors has proposed a new theory on secondary extinction (Kato, 1976, 1979, 1980, 1982). The present paper is written for two purposes. The first is to calculate numerically the extinction factor for spherical crystals, which are often used for accurate determination of crystal structures. So far, the calculation has been made only for parallel-sided crystals (Kato, 1980), for simplicity. For finite crystals like a cylinder and a sphere, the application of the simplest solution of the energy transfer equations in the Laue cases is insufficient to obtain the diffracted intensity for the whole crystal, because the optical paths in the Bragg cases and other geometrical cases are involved. In the present calculation, the correction is made approximately by using the rigorous solutions available for trapezoidal crystals. Not only the numerical values for a discrete set of parameters $\mu_0 R$, σR and θ_B, but also an analytical fitting function will be presented. Here, R is the radius of the crystal and σ is the coupling constant of the basic energy transfer equations. μ_0 and θ_B are the normal absorption coefficient and the Bragg angle, respectively. So far, to our knowledge, no such universal function has been presented.

The second aim is to illustrate the numerical difference between the conventional and present theories. Again, so far, it has been demonstrated only for parallel-sided crystals (Kato, 1982). Then, a significant discrepancy of more than 10% was noticed when the extinction factor was less than about 25%. A similar result is obtained here for spherical crystals.

2. The theoretical basis

In order to obtain the fundamental equation to describe secondary extinction the following energy transfer equations (ETE) are assumed (Kato, 1976).

$$\frac{\partial I_0}{\partial s_0} = -\mu_e I_0 + \sigma I_g \qquad (1a)$$

$$\frac{\partial I_g}{\partial s_g} = -\mu_e I_g + \sigma I_0, \qquad (1b)$$

where I_0 and I_g are the total intensities carried by the direct (O) and Bragg-reflected (G) beams. They

0567-7394/83/030305-06$01.50

propagate along the directions $\mathbf{s}_0$ and $\mathbf{s}_g$, respectively. μ_e is the effective absorption coefficient defined by

$$\mu_e = \mu_0 + \sigma. \tag{2}$$

The coupling constant σ in (1) and (2) has the form

$$\sigma = 2\tau_2/\Lambda^2, \tag{3}$$

where τ_2 is the correlation length of the lattice phase factor [equation (2), Kato (1976)] and Λ is the extinction distance.*

The following boundary conditions are assumed for solving (1).

$$I_g(s_0,0) = (1/\Lambda^2)\, E_e \exp -\mu_e s_0 \tag{4a}$$

$$I_0(0,s_g) = 0, \tag{4b}$$

where E_e is the total incident energy per unit time at the entrance point. Henceforth, it is assumed to be unity. The justification for the boundary conditions (4) is discussed in a previous paper (Kato, 1980). If the dynamical parallelepiped (DPE) effective at the observation point (s_0,s_g) is not truncated by other crystal surfaces (Fig. 1*a*), the solution of (1) is given by†

$$I_g^L = (1/\Lambda^2)\, I_0[2\sigma(s_0 s_g)^{1/2}] \exp -\mu_e(s_0 + s_g), \tag{5}$$

where I_0 is the modified Bessel function of zeroth order. Expression (5) is called the formula of the Laue case in this paper. When the DPE is truncated, one needs to subtract another term from I_g^L, because the beam paths passing through the protruding part of the DPE have to be excluded from the calculation. The dotted paths in Fig. 1 are the examples. The two cases, *B*I and *B*II, illustrated by Figs 1(*b*) and (*c*) must be distinguished. As a whole, however, they are referred to the Laue–Bragg–Laue cases. If the truncation boundary is a straight line, the terms to be subtracted are given in the form

$$I_g^{BI} = (1/\Lambda)^2[p_0 p_g/(s_0 s_g - q_0 q_g)] \times I_2[2\sigma(s_0 s_g - q_0 q_g)^{1/2}] \exp -\mu_e(s_0 + s_g) \tag{6a}$$

$$I_g^{BII} = (1/\Lambda)^2 I_0[2\sigma(s_0 s_g - q_0 q_g)^{1/2}] \exp -\mu_e(s_0 + s_g), \tag{6b}$$

where I_2 is the modified Bessel function of second order and the meanings of p_0, p_g, q_0 and q_g are shown in Figs. 1(*b*) and (*c*).

The case *B*I reduces to special cases; *i.e.* the Laue–Bragg ($q_0 = 0, p_0 = s_0$), the Bragg–Laue ($q_g = 0$, $p_g = s_g$) and the Bragg cases ($q_0 = q_g = 0$, $p_0 = s_0$, $p_g = s_g$). Mathematically speaking, the expressions for these cases have been obtained in wave-optics dynamical theory by Saka, Katagawa & Kato (1972*a*,*b*, 1973). If one replaces $(\kappa_g \kappa_{-g})^{1/2}$ by $i\sigma$, the results (6) can be derived. The simpler derivation will be reported elsewhere.

The integrated intensity for a finite convex crystal is given by

$$R_g = \lambda(\sin 2\theta_B)^{-2} \iiint I_g(E,A)\, \mathrm{d}X_E\, \mathrm{d}X_A\, \mathrm{d}Y, \tag{7}$$

where E and A are referred to the entrance point and the exit point, respectively. $I_g(E,A)$ is the angularly integrated intensity for a pair of E and A. In the Laue case, for example, (5) can be used for $I_g(E,A)$. The integral elements $\mathrm{d}X_E$ and $\mathrm{d}X_A$ are taken perpendicular to the direct (O) and the Bragg-reflected (G) beams, respectively, in the reflection plane and $\mathrm{d}Y$ is perpendicular to $\mathrm{d}X_E$ and $\mathrm{d}X_A$.

The extinction factor is defined by

$$\eta \equiv R_g/R_g^K, \tag{8}$$

where R_g^K is the kinematical integrated intensity per unit intensity of the incident beam in non-absorbing crystals. It is given immediately from (7) in the form

$$R_g^K = (\lambda/\sin 2\theta_B)\, \Lambda^{-2}\, V \equiv QV, \tag{9}$$

* $\Lambda^{-1} = r_c(\lambda/v)|F_g|C$. λ is the wavelength, v is the volume of the unit cell, r_c is the classical radius of the electron, $|F_g|$ is the structure factor, C is the polarization factor. In this paper, $|F_g| = |F_{-g}|$ is assumed.

† The expression for the direct beam is given by Kato (1976).

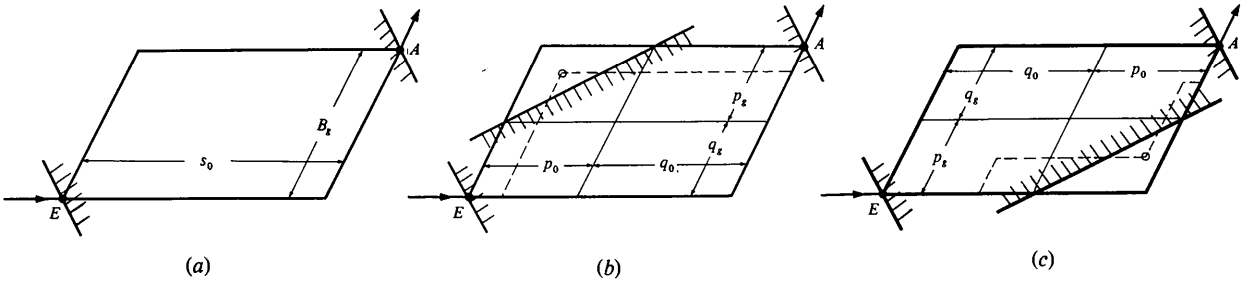

(*a*) (*b*) (*c*)

Fig. 1. The three cases of the truncation of the part of the crystal effective in the dynamical diffraction. (*a*) No truncation, (*b*) the case of *B*I, (*c*) the case of *B*II.

where V is the volume of the crystal.* The absorption factor is defined by

$$A = \int_V \exp -\mu_0(s_0 + s_g)\,dv, \qquad (10)$$

the integration being taken over the crystal.

3. Numerical calculation of the extinction factor

In this section, the procedures are outlined when neglecting the truncation of the DPE, so that (5) is used for $I_g(E,A)$. The correction due to the truncation will be explained in the next section.

Cylinder: The axis of the cylinder is assumed to be perpendicular to the reflection plane. The integrated intensity must be a function of $\alpha = (\mu_0 + \sigma)R, \beta = \sigma R$ and the Bragg angle θ_B, where R is the radius of the cylinder. For this reason, R_g values were calculated for a discrete set of three variables of α, β and θ_B. The ranges of calculation and the intervals are listed in Table 1. The integration in (7) is essentially two-dimensional, dY being redundant in this case. Simpson's method was used in the numerical integration.

Sphere: Similarly to the case of the cylinder, the extinction factors were calculated at a set of discrete values of α, β and θ_B listed in Table 1. Obviously, a single η value can be obtained by the three-dimensional integration. In practice, however, the results of the cylindrical case were stored in the data file and the Lagrange interpolation method was employed for calculating $R_g(Y)$ for every circular section specified by the parameter Y. Thus, the integration was essentially one-dimensional.

For the sake of cross checking, the three-dimensional integration was carried out directly with (7) at a few sets of α, β and θ_B values. It was confirmed that the agreement between the η values calculated by the different methods was better than 0·5‰.

* Note that the volume element is $dv = (\sin 2\theta_B)\,dX_E\,dX_A\,dY$.

Table 1. *The range and interval of the numerical calculation*

$\sigma R = \beta$	0·0 ~ 2·0; 0·1
$\mu_0 R = \alpha - \beta$	0·0 ~ 3·0; 0·1
θ_B	0·0 ~ 30°; 2·5°

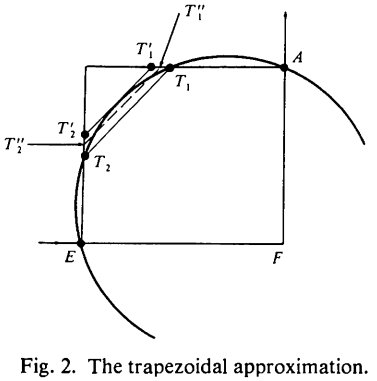

Fig. 2. The trapezoidal approximation.

4. The correction for the truncation of the DPE

Here, the procedures are explained in detail for the case of *B*I. The same procedures were applied also to *B*II. First, we consider the case of the cylinder. If the DPE of a pair of E and A is truncated by the arc T_1T_2 (Fig. 2), the crystal is approximated by the trapezoid $EFAT_1T_2$. Then, the correction (subtraction) term can be obtained with (6*a*) for $I_g(E,A)$ of (7). This term is called the first-stage correction.

Obviously, now, the correction is overestimated because the part of the crystal between the arc T_1T_2 and the straight line T_1T_2 is ignored. At the second stage, therefore, we took the trapezoid $EFAT_1'T_2'$, where $T_1'T_2'$ is the tangent of the cylinder parallel to T_1T_2. The true correction must lie between the corrections of the first and second stage.

Finally, partly for this reason but with intuition, we took the trapezoid $EFAT_1''T_2''$, which has the same volume of crystal as $EFAT_1T_2$. Again, $T_1''T_2''$ is parallel to the line T_1T_2. Table 2 shows the numerical examples of the correction of each stage for $\mu_0 R = 0$. The correction is significant for larger values of σR and θ_B. Fig. 3 shows the $\mu_0 R$ dependence of the correction

Table 2. *Examples of the trapezoidal approximation* ($\mu_0 R = 0$); *cylindrical crystals*

Parameter		$\sigma R = 1·0$ $\theta_B = 15°$	$\sigma R = 2·0$ $\theta_B = 15°$	$\sigma R = 1·0$ $\theta_B = 30°$	$\sigma R = 2·0$ $\theta_B = 30°$
η		0·3032	0·1659	0·3306	0·1934
$\Delta\eta$	stage I	0·0003	0·0007	0·0054	0·0096
	stage II	0·0001	0·0003	0·0026	0·0046
	stage III	0·0002	0·0004	0·0035	0·0055

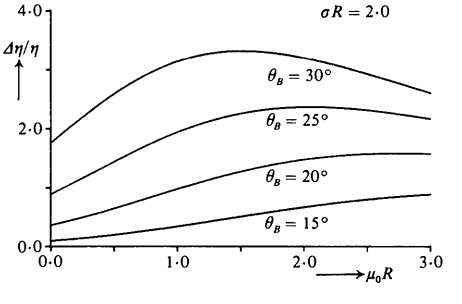

Fig. 3. The final correction in percentage of η.

in percentage of η. For smaller $\mu_0 R$, it increases with $\mu_0 R$ because η decreases more rapidly than the correction, which is essentially the surface effect. For larger $\mu_0 R$, however, the correction decreases with $\mu_0 R$. In this case, the diffraction is essentially kinematical, whereas the correction is required when multiple reflections are predominant. For this reason, the correction becomes less significant for larger $\mu_0 R$. The validity of the trapezoidal approximation explained here will be discussed in § 6.

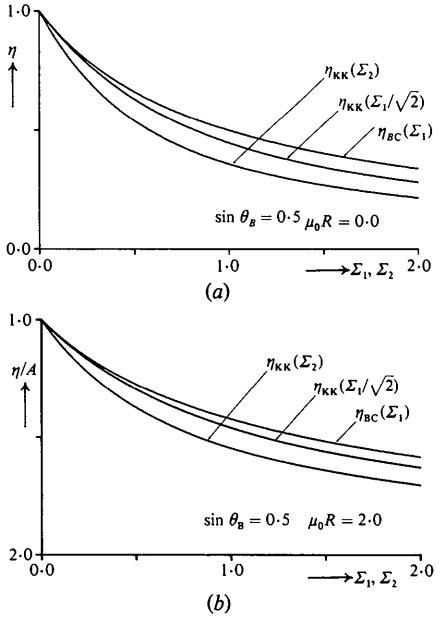

Fig. 4. Comparison between the calculations of Becker & Coppens and those of the present work for η/A: (*a*) $\sin\theta = 0{\cdot}5$, $\mu_0 R = 0{\cdot}0$; (*b*) $\sin\theta = 0{\cdot}5$, $\mu_0 R = 2{\cdot}0$, $\Sigma_1 = \sqrt{2}\sigma R$, $\Sigma_2 = \sigma R$.

It is straightforward to apply the above calculation to the spherical crystal. The procedures are the same as those explained in § 3 for the main term.

The extinction factors were recalculated with the use of the final corrections. Examples are shown as the curves denoted by η_{KK} in Fig. 4.

5. The functional fitting

For practical uses of the present calculation, it is desirable to represent η as an analytical function of three parameters, α, β and θ_B. Then, extinction correction can be practised easily in structure analysis. After a few trials, it was found that the following expression was useful both for cylindrical and spherical crystals.

$$\eta = \exp\{-[C\alpha + D(\theta)\alpha^2 + G(\theta)\beta^2]\} \times \exp\left[\sum_{l,m,n} c_{l,2m,n}\alpha^l \beta^{2m}\cos^n(2\theta_B)\right]. \quad (11)$$

Table 3. *The coefficients of the cumulant factor*

Cylinder

$D_0 = -5{\cdot}898306 \times 10^{-2}$	$G_0 = -0{\cdot}4999730$
$D_1 = -2{\cdot}553589 \times 10^{-5}$	$G_1 = -2{\cdot}554632 \times 10^{-5}$
$D_2 = -5{\cdot}403935 \times 10^{-10}$	$G_2 = -4{\cdot}678440 \times 10^{-10}$
$D_3 = 7{\cdot}100944 \times 10^{-14}$	$G_3 = 6{\cdot}156740 \times 10^{-14}$

Sphere

$D_0 = -0{\cdot}1111103$	$G_0 = -0{\cdot}3333212$
$D_1 = -1{\cdot}701235 \times 10^{-5}$	$G_1 = -1{\cdot}701113 \times 10^{-5}$
$D_2 = -3{\cdot}646856 \times 10^{-10}$	$G_2 = -3{\cdot}249776 \times 10^{-10}$
$D_3 = 4{\cdot}828941 \times 10^{-14}$	$G_3 = 4{\cdot}337572 \times 10^{-14}$

Table 4. *The least-squares coefficients of the remainder factor*

Cylinder

*c*300	*c*120	*c*400	*c*220	*c*040	*c*500	*c*320	*c*140
0·0518655	−0·575144	−0·0185806	0·154378	0·0425078	0·00361003	−0·0215008	−0·0049286
*c*301	*c*121	*c*401	*c*221	*c*041	*c*501	*c*321	*c*141
−0·00983204	0·806559	−0·0101829	−0·320742	−0·0689021	−0·00751437	0·0733876	−0·0150964
*c*302	*c*122	*c*402	*c*222	*c*042	*c*502	*c*322	*c*142
0·00348695	−0·410757	0·0724167	0·132462	0·0421504	0·00250727	−0·0708694	0·0478474
*c*303	*c*123	*c*403	*c*223	*c*043	*c*503	*c*323	*c*143
−0·0336315	0·105244	−0·0433543	0·0270721	−0·0338989	0·00126424	0·0195296	−0·0224710

Max. deviation 0·787%
Standard deviation 0·437%

Sphere

*c*300	*c*120	*c*400	*c*200	*c*040	*c*500	*c*320	*c*140
0·0905622	−0·633457	−0·0543295	0·251772	0·0373821	0·00817658	−0·0344214	−0·00941525
*c*301	*c*121	*c*401	*c*221	*c*041	*c*501	*c*321	*c*141
−0·276338	1·44013	0·177331	−0·823258	−0·0828162	−0·0299750	0·132249	0·0191922
*c*302	*c*122	*c*402	*c*222	*c*042	*c*502	*c*322	*c*142
0·384142	−1·48413	−0·212689	0·940510	0·0712921	0·0370758	−0·164276	−0·00936756
*c*303	*c*123	*c*403	*c*223	*c*043	*c*503	*c*323	*c*143
−0·188864	0·596664	0·0887762	−0·368624	−0·0331277	−0·0153002	0·0668285	0·00208394

Max. deviation 0·436%
Standard deviation 0·177%

The first factor is called the cumulant factor, which ensures fitting to the calculated values for small α and β. The second factor is called the remainder, which is introduced for better fitting within the range of calculation.

From the definition (7) of the integrated intensities R_g, it is expected generally that η must be an even function of β and θ_B. The right side of (11) meets this requirement.

For finding the cumulant coefficients, (5) is assumed for $I_g(E,A)$ in (7), for simplicity. Then, it turns out that

$$C = \langle s_0 + s_g \rangle = \tfrac{16}{3}\pi \text{ (cylinder)} \qquad (12a)$$

$$= \tfrac{4}{3} \quad \text{(sphere)} \qquad (12b)$$

$$D = \tfrac{1}{2}C^2 - \tfrac{1}{2}\langle (s_0 + s_g)^2 \rangle \qquad (12c)$$

$$G = -\langle s_0 s_g \rangle, \qquad (12d)$$

where $\langle\ \rangle$ implies the average over the crystal. The coefficients D and G must be angular-dependent so that they are developed in the form of power series of θ_B in degrees:

$$D(\theta_B) = D_0 + 4D_1\theta_B^2 + 16D_2\theta_B^4 + 64D_3\theta_B^6 \qquad (13a)$$

$$G(\theta_B) = G_0 + 4G_1\theta_B^2 + 16G_2\theta_B^4 + 64G_3\theta_B^6. \qquad (13b)$$

The left-hand sides were calculated numerically from (12). Based on these results, the coefficients D_l and G_l were determined by least squares. They are listed in Table 3.

The next problem is to find the coefficients in the rest of (11). The terms in the exponent were limited by imposing the conditions

$$3 \le l + 2m \le 5, \quad 0 \le n \le 3 \qquad (14a,b)$$

on the indices. Including the terms of higher orders did not improve effectively the fitting. For describing the angular dependence $\cos 2\theta_B$ was used instead of θ_B^2 merely as an empirical reason to attain better results. The 32 coefficients, in total, were determined by least squares in three-dimensional space. The results are listed in Table 4. In this calculation, of course, η values including the correction of stage III were employed. The maximum deviation in fitting was 0·79 (cylinder) and 0·44% (sphere) of η, provided that η is larger than 0·1.

6. Discussion and conclusions

6.1. *The accuracy of the present calculation*

The numerical error ($\Delta\eta$) due to computation was set to be ess than 1‰ of η. In the case of the functional fitting, the maximum deviation was confirmed to be less than 0·4% of η. The formula (11), therefore, should be used with this accuracy. For work requiring higher accuracy, it is recommended to file a set of computed values of η and to use Lagrange interpolation.

It is not easy to evaluate precisely the accuracy of the trapezoidal approximation described in § 4. The true value of the correction for the truncated DPE must be between the corrections of stages I and II. The maximum estimation of the error, therefore, is the difference of the relevant two figures listed in Table 2. $\Delta\eta/\eta$ amounts to a few percent in the worst case.

Obviously, the above estimation is rough and excessive. Fortunately, Hamilton (1963) reports a numerical solution of the recurrence formulae equivalent to (1) in the case of non-absorbing cylindrical crystals. The agreement between his results and ours is better than 2‰ within the domain of our calculation. For this reason, it is reasonable to take this figure as a measure of accuracy of the present calculation with a safety margin. We, however, believe that the present calculation could be used with accuracy of 1‰ from the numerical analysis of the correction term.

It must be emphasized that the correction for the truncation of the DPE is necessary for any work which requires accuracy better than a few percent in structure factors. In this respect, the results of Becker & Coppens (1974) are not correct.

6.2. *The comparison between the present and traditional theories*

The following has been discussed by one of the present authors (Kato, 1982) in the simplest case of parallel-sided crystals. Here, it is shown that similar conclusions are obtained also in the case of spherical crystals.

According to the new theory of secondary extinction, two tasks have to be distinguished. One is to obtain the extinction function $\eta(\alpha,\beta,\theta_B)$. The principal part of the present work is this task for cylindrical and spherical crystals. Another is to find the coupling constant σ or, more precisely speaking, the correlation length τ_2 based on the model of crystal textures. Incidentally, the function $\eta(\alpha,\beta,\theta_B)$ is model-independent.

The simple and popular model of the texture is 'mosaic crystals'. Optically speaking, however, 'coherent domain model' would be appropriate so that 'mosaic crystallites' in the traditional usage is replaced by 'coherent domain'. With this model, τ_2 can be calculated as follows (Kato, 1982):

$$\tau_2 = \tfrac{1}{2}\int_{-\infty}^{+\infty} \{Z(\xi)\}^2\,\mathrm{d}\xi, \qquad (15)$$

where

$$Z(\xi) = \frac{2}{\pi}\int_{-\infty}^{+\infty} \Phi(\varphi)\,\mathrm{d}\varphi \int_0^{\infty} L(l)\,\frac{\sin\{(\xi + \alpha\varphi)\,l\}}{\xi + \alpha\varphi}\,\mathrm{d}l \qquad (16)$$

is the Fourier transform of the correlation function $f(z)$ of the lattice phase factors. Here, $\Phi(\varphi)$ is the

normalized distribution function of the coherent domains and $L(l)$ is the normalized distribution function of half of the domain size, l.

The model must be specified further by taking any specific distributions of $\Phi(\varphi)$ and $L(l)$. For example, one can take

$$\Phi(\varphi) = \sqrt{2}g \exp\{-2\pi g^2 \varphi^2\} \tag{17a}$$

$$L(l) = \frac{\pi}{2}(l/\bar{l}^2) \exp\{-(\pi/4)(l/\bar{l})^2\},* \tag{17b}$$

where $\bar{l}$ is the mean value of l. Then, one obtains

$$\tau_2 = (\bar{l}/\sqrt{2})(1 + 2x^2)^{-1/2}, \tag{18}$$

where

$$x = (\sin 2\theta_B/\lambda)\bar{l}/g. \tag{19}$$

The conventional theory has a different theoretical scheme from the present one. The extinction factor η is a *functional* of $\Phi(\varphi)$ and $L(l)$, in general. Becker & Coppens (1974) avoid this complexity by assuming some *ad hoc* treatments. For example, the domain size is assumed to be spherical and the averaged diffraction function in intensity, $\bar{\sigma}(\xi + \alpha\varphi)$, of the coherent domain is assumed Gaussian or Lorentzian without any justification. Nevertheless, finally, they obtained the expression for η as a function of x defined by (19) for a Gaussian distribution of $\Phi(\varphi)$ and $\bar{\sigma}(\xi + \alpha\varphi)$.

In order to compare their numerical results with ours, we shall write their extinction factor for the Gaussian distributions of $\Phi(\varphi)$ and $\bar{\sigma}(\varphi)$ in the form

$$\eta_{BC} = \eta_{BC}(\Sigma_1, M, \theta_B), \tag{20}$$

where

$$\Sigma_1 = (\bar{l}R/A^2)(1 + 2x^2)^{-1/2}, \quad M = \mu_0 R. \tag{21a,b}$$

The functional form η_{BC} is drawn in Fig. 4. The present results [(3) and (18)] give the numerical values of η in the form

$$\eta_{KK} = \eta_{KK}(\Sigma_2, M, \theta_B), \tag{22}$$

* $\int_0^\infty dl$ in (16) gives the Gaussian distribution of $\xi + \alpha\varphi$.

Table 5. *A comparison between the Becker & Coppens (1974) and the present results*

	$\Delta\eta/\eta$ (in %)					
$\mu_0 R$	0·0	0·0	1·0	1·0	2·0	2·0
$\sin\theta$	0·2	0·5	0·2	0·5	0·2	0·5
η						
0·8	1	1	1	1	3	3
0·6	5	6	5	5	9	8
0·4	13	14	13	11	17	—

where

$$\Sigma_2 = \Sigma_1/\sqrt{2}. \tag{23}$$

By changing the scale of ordinate from Σ_2 to Σ_1, Fig. 4 includes the curves of $\eta_{KK}(\Sigma_1/\sqrt{2})$, which should be compared with $\eta_{BC}(\Sigma_1)$.*

With this analysis, it is concluded that $\eta_{BC}(\Sigma_1) > \eta_{KK}(\Sigma_1/\sqrt{2})$. The disagreement increases with Σ_1. The percentage differences are listed in Table 5. The difference is significant unless the extinction is less than about 20%.

Finally, one remark is mentioned. So far, we have used the terminology of 'extinction factor' to include the absorption effect. As is easily seen from the physical meanings of extinction and absorption, the 'extinction factor' must be a function of σR, $(\sigma + \mu_0)R$ and θ_B. For this reason, the present treatment is more reasonable than the traditional treatment, in which the absorption and extinction factors are treated separately.

* M and θ_B are dropped.

References

BECKER, P. J. & COPPENS, P. (1974). *Acta Cryst.* A**30**, 129–147.

HAMILTON, W. C. (1963). *Acta Cryst.* **16**, 609–611.

KATO, N. (1976). *Acta Cryst.* A**32**, 458–466.

KATO, N. (1979). *Acta Cryst.* A**35**, 9–16.

KATO, N. (1980). *Acta Cryst.* A**36**, 171–177.

KATO, N. (1982). *Z. Naturforsch. Teil A*, **37**, 485–489.

SAKA, T., KATAGAWA, T. & KATO, N. (1972*a*). *Acta Cryst.* A**28**, 102–113.

SAKA, T., KATAGAWA, T. & KATO, N. (1972*b*). *Acta Cryst.* A**28**, 113–120.

SAKA, T., KATAGAWA, T. & KATO, N. (1973). *Acta Cryst.* A**29**, 192–200.